DIFFRACTION GRATING SCANNERS USING POLYSILICON MICROMOTORS

A.A. Yasseen, S.W. Smith, M. Mehregany, and F.L. Merat

Electronics Design Center
Department of Electrical Engineering & Applied Physics
Case Western Reserve University,
Cleveland, Ohio 44106, USA

Abstract

This paper describes polysilicon micromotors with diffraction gratings fabricated on the polished surface of the polysilicon rotor for optical scanning applications. Such micromotor optical scanners have high quality scan profiles, good efficiency, meter working distances, and multiple out of plane beam diffraction orders. Above all, the scanner design takes full advantage of planar processing. Chemical-mechanical polishing is used to reduce the polysilicon rotor's average surface roughness (Ra) from 420Å to below 17Å, improving the optical performance of the grating fabricated on the rotor. The gratings are tested at visible wavelengths (633nm) and are verified to have spatial periods of 1.80μm and 3.86μm, closely matching their design. The microscanners can be operated at voltages as low as 18V, with a maximum operational speed of 1100 rpm (limited by the driving electronics). Preliminary bar code scanning is demonstrated without an external lens system.

1 Introduction

In [1], we presented polygon microscanners using polysilicon micromotors, whose rotor carried a high-aspect-ratio reflective electroless plated nickel polygon. Reflection from the nickel polygon side wall was used for scanning. This paper describes a planar diffraction grating scanner incorporating a reflective grating on the rotor of a polysilicon micromotor. This design requires the fabrication of micromotors with large-area solid disk rotors, as well as chemical-mechanical polishing (CMP) of the polysilicon rotor surface for improved feature definition and optical characteristics. By eliminating the need for high aspect ratio lithography and nickel plating for polygonal micromotor scanners as reported in [1], the fabrication process can be fully implemented in polysilicon surface micromachining. Planar optical elements allow greatly simplified optical alignment and packaging in comparison to their polygonal counterparts. In comparison, the grating micromotor scanners benefit from low cost batch fabrication, high rotation speeds, and small size. Their IC compatibility permits integration with on-chip drive and control electronics. Applications include bar code scanners, high speed optical switches, multiplexers, and computer interconnects, among others.

2 Microscanner Design

Continuation of our previous microscanner work has resulted in the development of a grating micromotor scanner. The micromotors have planar single and pyramidal grating elements (i.e., an element consisting of four pie-shaped regions with adjacent regions having orthogonal line orientation) etched into the rotor with the grating spatial periods designed to be 2μm and 4μm. The grating etch depth is adjusted to maximize the intensity in a desired diffraction order for an incident light wavelength [2]. The diffraction grating patterns may be designed to produce multiple diffracted beams for scanning at different focal lengths and angles. Illuminated single element gratings produce a row of diffraction orders spaced at angles given by [3]:

$$\theta_q = \theta_i + q\frac{\lambda}{\Lambda};\ q = 0,\pm1,\pm2,\ldots$$

where θ_i denotes the angle of the incident beam relative to the normal, q the diffraction order, λ the wavelength of the incident light, and Λ the grating period. These gratings can operate in either transmission or reflection

 0-7803-2503-6

modes, thus adding an extra degree of freedom to the overall scanner design. Only reflection mode gratings are considered in this paper, however. A multifacet pyramidal grating as described above can yield two perpendicular rows of diffraction orders. As the scanner rotates, concentric scanned arcs are produced by the various diffraction orders, each of which may be used for scanning. Both wobble and salient-pole motors are produced, but the focus of this paper is on salient-pole micromotors as they operate at higher speeds than wobble micromotors. The motors have solid polysilicon rotors with diameters in the range 0.5 to 2mm for both salient pole and wobble micromotor designs. Figure 1 shows an SEM photograph of a typical diffraction grating microscanner.

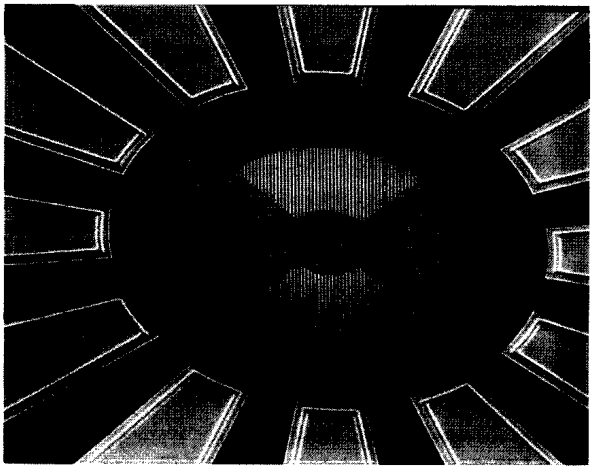

Figure 1: A typical 500μm-diameter salient-pole micromotor scanner with polished rotor/stator polysilicon and pyramidal grating element of 1.80μm period.

3 Fabrication of the Microscanners

Device fabrication is based on a five mask process which is an extension of the three mask process described in [4]. Figure 2 presents a schematic description of the scanner fabrication process. Initially, 4500Å of LPCVD silicon nitride for electrical isolation followed by 3.5μm of PSG for a sacrificial layer are deposited. The stator and the bearing post anchors are then patterned, followed by a 5.5μm thick rotor/stator LPCVD polysilicon deposition and subsequent heavy doping with phosphorous. Thick (e.g., 5.5μm) polysilicon rotor/stator films are required to provide sufficient mechanical stiffness and to prevent out-of-plane warping of large area rotors. With increasing LPCVD polysilicon thickness, the film roughness increases. Longer diffusion times are also needed to subsequently dope the polysilicon, further increasing the surface roughness. This inherent polysilicon surface roughness results in two limitations: (i) feature size definition and quality degradation; and (ii) undesirable optical scattering.

To produce high quality optical surfaces, the average polysilicon surface roughness (Ra) should be reduced to at least below 20Å. Fabrication of diffraction gratings also requires stringent line width and spacing control during photolithography and pattern delineation to obtain satisfactory optical performance. To meet these requirements, we used CMP to polish the surface of the polysilicon rotors on which the gratings are fabricated. Process simplicity, low cost per wafer, and the potential to produce a smooth, damage-free surface for subsequent device processing are some of the reasons for the increasing use of CMP in IC processing. By adjusting the chemical and mechanical components, CMP can be readily tailored to virtually any IC compatible material.

We have used CMP to eliminate the surface roughness inherent to polysilicon films. With CMP, the average polysilicon surface roughness (Ra) of our 5.5μm-thick polysilicon films on which the gratings are fabricated is reduced from 420Å to below 17Å (with less than 1500 Å film removal). Figure 3 demonstrates the significant feature size definition and quality (e.g., sidewall smoothness) improvement, as well as the substantial surface roughness reduction, for polished versus unpolished films. Subsequent to CMP of the rotor/stator polysilicon, the gratings are patterned and etched (~0.5μm deep) into the polysilicon layer using an isotropic dry etch in order to approximate a sinusoidal grating profile for high optical diffraction efficiency. Figure 4 shows SEM profiles of gratings fabricated on polished and unpolished polysilicon. Next, the rotor/stator pattern is defined and delineated using a

highly anisotropic dry etch to produce 1μm rotor/stator gaps. The flange mold is then defined and etched, followed by a 0.3μm bearing clearance oxidation. A 1.2μm-thick polysilicon layer is deposited by LPCVD and patterned to produce the bearing.

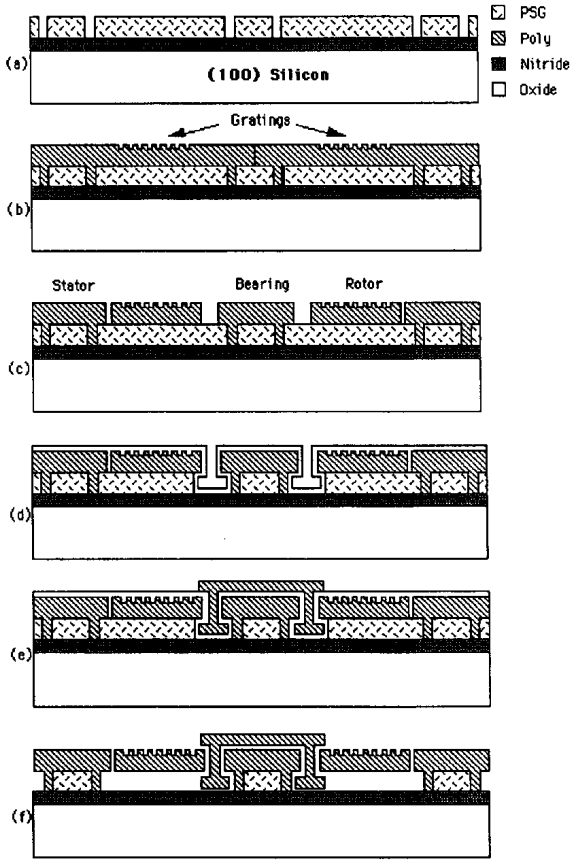

Figure 2: Cross-sectional schematics describing the microscanner fabrication process: (a) after anchor definition and patterning; (b) grating definition and patterning; (c) rotor/stator definition and patterning; (d) bearing clearance oxidation; (e) bearing definition and patterning; and (f) released device.

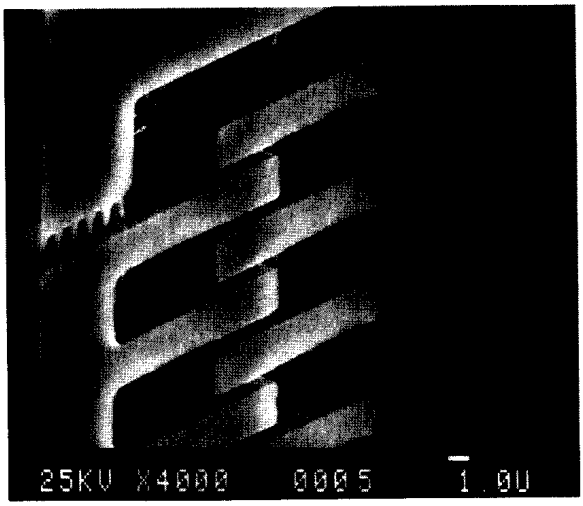

(a)

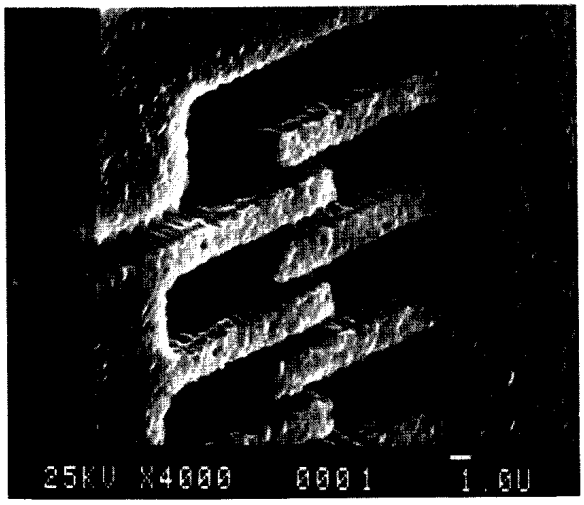

(b)

Figure 3: Close-up view of polysilicon comb fingers fabricated in (a) unpolished and (b) polished 3.5μm-thick polysilicon. Note the improved feature definition, side wall quality, and line width resolution, as well as polysilicon surface roughness.

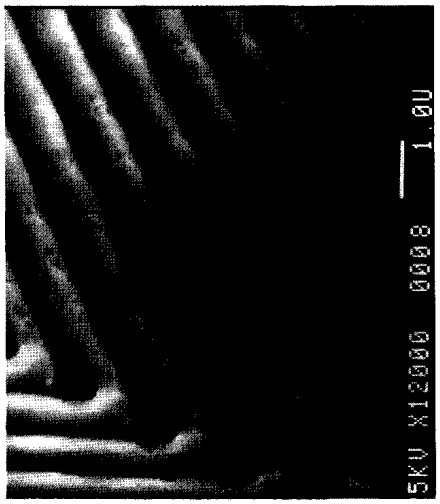

(a)

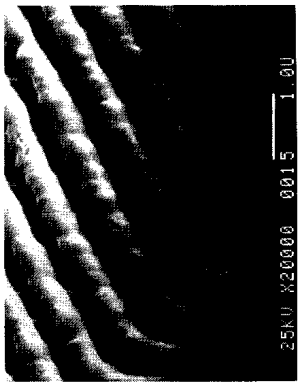

(b)

Figure 4: Close-up view of 1.80μm spatial period diffraction gratings fabricated in (a) polished and (b) unpolished polysilicon.

4 Polysilicon Diffraction Microscanners

The optical properties of reflective diffraction gratings fabricated on polished and unpolished polysilicon rotors demonstrate the importance of polishing the rough polysilicon surface for optical applications. Figure 5 demonstrates that CMP reduced the undesirable light scattering due to the excessive polysilicon surface roughness to values comparable to that achieved for gratings on single crystal silicon wafers. For comparison, gratings are etched into single crystal silicon wafers, in addition to polished and unpolished polysilicon surfaces.

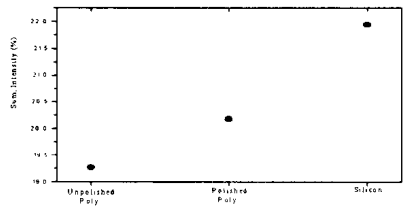

Figure 5: Sum of intensity from all diffraction orders from gratings fabricated on polished and unpolished polysilicon, as well as single-crystal silicon wafers.

The grating periods of the nominally 2 and 4μm gratings are measured (using a He-Ne laser of 633nm wavelength) to be 1.80 and 3.86μm, respectively. This result is in close correspondence with the target design and the difference is attributed to variations in timed etching and photolithography. The grating etch depth can be adjusted to maximize intensity in a desired diffraction order (e.g., typically the first order) for a given incident optical wavelength. Figure 6 demonstrates that adjusting the grating etch depth can be used to shift power from the zeroth order to higher diffraction orders.

Characterization of the diffracted laser beam profiles with a CCD camera indicates that at distances on the order of one meter from the scanner all diffraction orders provide gaussian beam profiles, with gratings on polished polysilicon producing a higher degree of spatial uniformity and lower beam divergence than those on unpolished polysilicon. Figure 7 compares measured beam profiles on polished and unpolished polysilicon at a distance of 1m from the wafer. The measured diffraction orders for 1.80μm gratings are separated by 20.79°±0.62° and those for the 3.86μm gratings by 9.8°±0.53°. The line width and diffraction angles are uniform for similar gratings on the same wafer and between different wafers. Optical scanning at distances up to several meters without external optics is readily possible and demonstrated. The effects of small (0.5 mm diameter) motor size and extraneous motor features (i.e. 25 μm radius bearing) are found to be negligible upon the overall optical performance of the scanner.

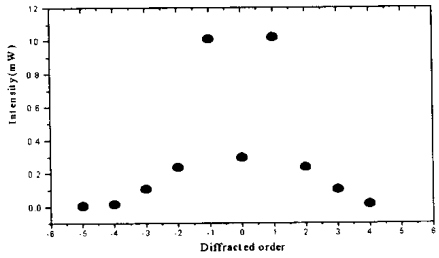

Figure 6: Diffraction orders for a 3.86μm period grating showing transfer of optical power from the zeroth to the first order spots.

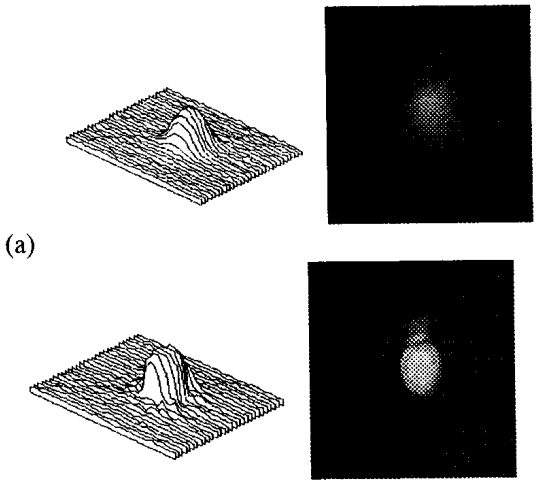

(a)

(b)

Figure 7: Beam intensity profiles (left) and spot quality (right) from similar gratings fabricated on (a) unpolished and (b) polished polysilicon rotors at 0.5 meter distance from a grating microscanner using 633nm light. Note the increased intensity and reduced beam divergence as a result of polishing.

The microscanners designed in this paper operate smoothly and reproducibly in room air for extended periods after release. Super-critical CO_2 [5] release is needed to permit the scanners to operate without stiction after release. Both 1 and 2 μm rotor/stator gap motors are operational. Minimum operating voltages are as low as 18V, while maximum rotor speeds have been 1100 rpm (limited by the driving electronics) for the salient-pole micromotor design and 23 rpm for the wobble micromotor design.

Scanning operation is demonstrated using a 633nm wavelength He-Ne laser incident on a salient-pole single element (one grating covering the entire rotor) microscanner with a 1.80μm grating period. Multiple diffraction orders are visible at meter distances. The scanned beams are examined with a silicon photodiode and a dynamic digital signal analyzer. The uniformity of the scanned beams are measured over many revolutions of the scanner. Figure 8 shows a typical intensity profile for a salient-pole microscanner during operation.

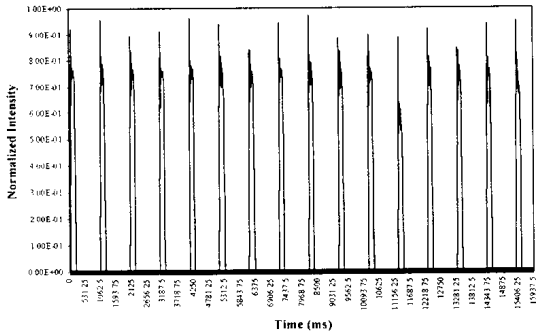

Figure 8: Typical scan intensity measured over several revolutions of the micromotor scanner. The 500μm-diameter salient-pole microscanner is turning at 60 rpm.

5 Bar Code Scanning Application

Bar code scanning using a microscanner is demonstrated as a typical application of this device. A simple test bar code, shown in Fig. 9, is illuminated by a laser beam diffracted by the grating microscanner. Figure 10 displays a typical photodiode signal resulting from scanning a 633nm He-Ne laser beam over the bar code pattern. The optical reflection from the bar code is detected by a silicon photodiode and a digital dynamic signal analyzer. No external lens system is used in the experiment with the grating microscanner. The peaks and valleys in the trace correspond to the light and dark areas of the bar code. The shape of this trace is dependent on many factors including motor speed, light intensity, relative positions of the bar code detector,

detector acceptance angle, and detector time constant. The detected signal can be improved by external optics to suit the requirements of many commercial bar code reading applications.

Figure 9: A test bar code with alternating light and dark periods with decreasing bar width and spacing.

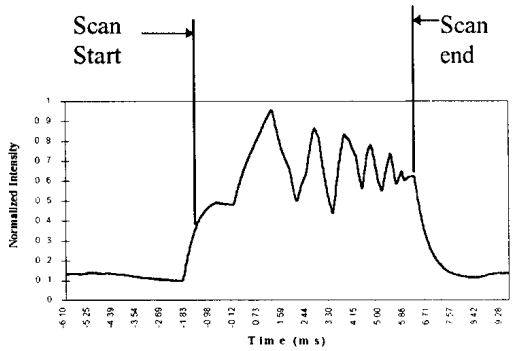

Figure 10: Scan of the test bar code in Fig. 9 using a grating microscanner. Note that the signal peaks correspond to the light areas and the valleys correspond to the dark areas of the bar code shown in Fig. 9.

6 Conclusion

Our results demonstrate laser beam scanning using diffraction element microscanners. CMP is shown to significantly improve the optical performance of diffraction elements fabricated on polysilicon micromotor rotors. The high quality diffraction beam profiles indicate that polished polysilicon is a viable material for production of low cost high quality micoscanners. Planar processing is also shown to have many advantages over high aspect ratio photolithography. Finally, we have demonstrated a typical application of the diffraction grating microscanner to bar code scanning.

Acknowledgment

The authors would like to thank Girish Ramanathan and Shuvo Roy, both of Case Western Reserve University, for assistance in micromotor dynamical testing and for comb patterns used in CMP evaluation, respectively. This work was supported in part by ARPA under Contract No. F49620-94-C-0007 and by NSF under Grant No. ECS-9109343.

References

[1]K. Deng, Tech. Dig., Solid-State Sensor & Actuator Workshop (Hilton Head, SC, June 1994), p. 234.

[2]O. Solgaard, et al., Optics Letters (Vol. 17, No. 9, May 1, 1992), p. 688.

[3]Gerakd F. Marshall, ed., Optical Scanning(New York: Marcel Dekker, Inc., 1991) 159.

[4]K. Deng, et al., Tech. Dig., 7th Int. Conf. on Solid-State Sensors & Actuators (Yokohama, Japan, June 1993), p. 756.

[5]G. T. Mulhern, et al., 7th Int. Conf. on Solid State Sensors & Actuators (Yokohama, Japan, June 1993), p. 296.